Selected Paper

Static and Dynamic Stereochemistry of Tris(9-triptycyl)stannane Derivatives#

Gaku Yamamoto,* Shozo Ohta, Megumi Kaneko, Kaoru Mouri, Miki Ohkuma, Ryo Mikami, Yosuke Uchiyama, and Mao Minoura

Department of Chemistry, School of Science, Kitasato University, Kitasato, Sagamihara, Kanagawa 228-8555

Received October 26, 2004; E-mail: gyama@kitasato-u.ac.jp

Static and dynamic stereochemistry of several tris(9-triptycyl)stannane derivatives Tp_3SnX (X = H, halogens, and alkyl groups) were studied. X-ray crystallography of the bromo and methyl compounds showed that the Sn atom was fundamentally tetrahedral and that the three Tp groups meshed with each other like bevel gears and formed a near-C_3 chiral conformation. The rate constants for enantiomerization of the chiral conformation in solution could be obtained by the lineshape analysis of the aromatic proton signals, even when a direct probe for enantiomerization such as a benzyl group was absent. The energy barrier to enantiomerization decreased as the substituent X became bulkier, suggesting that the ground state is more destabilized than the transition state upon introduction of a bulkier group.

Compounds in which two 9-triptycyl (Tp) groups are attached to a central atom X, Tp_2X, where X is CH_2, NH, O, SiH_2, and so on, show very interesting stereochemical behavior.[1] The two Tp groups are tightly meshed like bevel gears, and correlated disrotation of the two Tp–X bonds takes place with a very low energy barrier, while "slippage" of the gear, i.e., conrotation of the two Tp–X bonds, has a very high energy barrier. Therefore, when a benzene ring of each Tp group is suitably labeled, the phase relationship between the labeled benzene rings remains intact unless the gear slippage occurs; thus "phase" isomers are separately isolated if the energy barrier to the gear slippage is sufficiently high. Typical examples are given in Chart 1. The energy barriers to gearing could not be obtained experimentally, but were estimated by molecular mechanics calculations to be less than 4 kJ mol^{-1}.[1a] The barriers to gear slippage were obtained in terms of the isomerization barriers of the phase isomers: those for compounds given in Chart 1 were found to be 134.7, 163.6, and 175.7 kJ mol^{-1} for X = CH_2, NH, and O, respectively.[1a] The barrier heights are naturally highly dependent on the nature of the central atom X, the main factor being the Tp–X bond length. When X = SiH_2, phase isomers could no more be isolated and the NMR lineshape analysis gave the activation energy of 80 kJ mol^{-1} for the gear slippage.[1a]

It therefore seemed very intriguing to study the stereochemical behavior in compounds where three Tp groups are attached to a central atom X, i.e., Tp_3X.[1c] In these compounds, rotations around the Tp–X bonds necessarily involve disrotation of two Tp groups, i.e., gear slippage, and thus the energy barrier to any stereomutation involving the Tp–X rotations would be significantly high.

Molecular model considerations show that Tp_3X compounds are highly congested, especially when the central atom is of a low-period element such as C or N. Actually the only compounds of this type so far reported are chlorotris(9-triptycyl)germane (**1**) by Mislow and co-workers[1c,2] and chlorotris(9-triptycyl)stannane (**3**):[3] the latter was later shown to be impure.[2] Mislow and co-workers studied the stereochemistry of **1**.[2] They revealed by X-ray crystallography that **1** adopted gear-meshed chiral conformation. They resolved **1** into enantiomers using liquid chromatography with a chiral column at low temperatures, and found that racemization took place in methanol at −29 °C with $k = 5.33 \times 10^{-5}$ s^{-1} and $\Delta G^{\ddagger} =$ 79.4 kJ mol^{-1}. They did not however examine the mechanism of the racemization, nor did they study the lineshape analysis of the NMR spectra, although they found that compound **1** showed temperature-dependent NMR spectra.

We have recently developed a simple synthetic route to bromotris(9-triptycyl)stannane (**2**) and have succeeded in obtaining various derivatives of the general formula Tp_3SnX from **2**, among which are compounds **3**–**7** (Chart 2). We therefore decided to systematically study static and dynamic stereochemistry of these compounds, by X-ray crystallography to reveal the molecular structures in the crystalline state and by dynamic NMR spectroscopy to reveal the conformational inter-

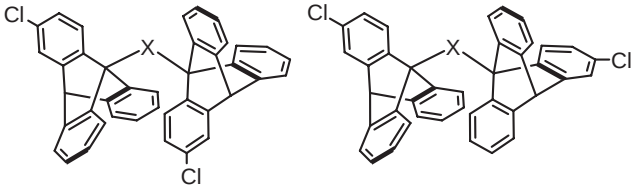

Chart 1.

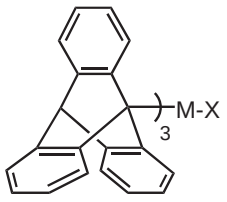

1: M = Ge, X = Cl
2: M = Sn, X = Br
3: M = Sn, X = Cl
4: M = Sn, X = F
5: M = Sn, X = CH_3
6: M = Sn, X = $CH_2C_6H_5$
7: M = Sn, X = H

Chart 2.

Published on the web March 11, 2005; DOI 10.1246/bcsj.78.487

conversion in solution. In this article, the synthesis, X-ray crystallography, and dynamic NMR studies of a series of halostannanes **2–4** and alkyl- and hydridostannanes **5–7** are reported and the stereochemical behavior of these compounds is discussed. Some of the preliminary results have been published.[4]

Results and Discussion

Syntheses. Bromotris(9-triptycyl)stannane (**2**) was obtained by treatment of a quarter molar amount of $SnBr_4$ with 9-triptycyllithium prepared from 9-bromotriptycene and butyllithium. A similar reaction of the 9-triptycyllithium with $SnCl_4$ gave a ca. 7:1 mixture of chlorotris(9-triptycyl)stannane (**3**) and the bromo compound **2**, and the isolation of **3** in a pure state was quite difficult as noticed by Mislow et al.[2] However, pure **3** was obtained by lithiation of **2** with *t*-butyllithium to give tris(9-triptycyl)stannyllithium (**8**), followed by treatment of **8** with SO_2Cl_2. Fluorotris(9-triptycyl)stannane (**4**) was obtained by reaction of **2** with KF in the presence of 18-crown-6. Methyltris(9-triptycyl)stannane (**5**) and benzyltris(9-triptycyl)stannane (**6**) were synthesized by alkylation of **8** with methyl iodide and benzyl bromide, respectively. Tris(9-triptycyl)stannane (**7**) was prepared by reducing **2** with $LiAlH_4$/$AlCl_3$.

X-ray Crystallography. Structural analysis by X-ray diffraction was performed for single crystals of compounds **2** and **5**. The perspective drawings of the molecular structures of these compounds are shown in Fig. 1. Representative bond lengths and angles are compiled in Table 1. In either compound, the molecule adopts a chiral conformation with the Sn–X bond as an approximate C_3 axis, where three Tp groups tightly intermesh with one another.

Table 1 shows that the Sn atom is tetrahedral in all the compounds, though significantly distorted. The C–Sn–C angles (av. 115°) are larger and the x–Sn–C angles (av. 103°; x denotes the central atom in group X) are smaller than the tetrahedral value of 109.5°, suggesting large steric repulsion among the Tp groups. The Sn–C bond lengths are 2.29–2.33 Å, significantly larger than the normal value (e.g., 2.144 Å for tetramethylstannane).

The three Tp–Sn bonds are twisted from a regular staggered conformation to similar extents. The three benzene rings in a Tp group have dihedral angles of ca. ±30, ∓90, and ±150° against the Sn–X bond axis (i.e., +30, −90, and +150° in the *P* conformer[5] and −30, +90, and −150° in the *M* conform-

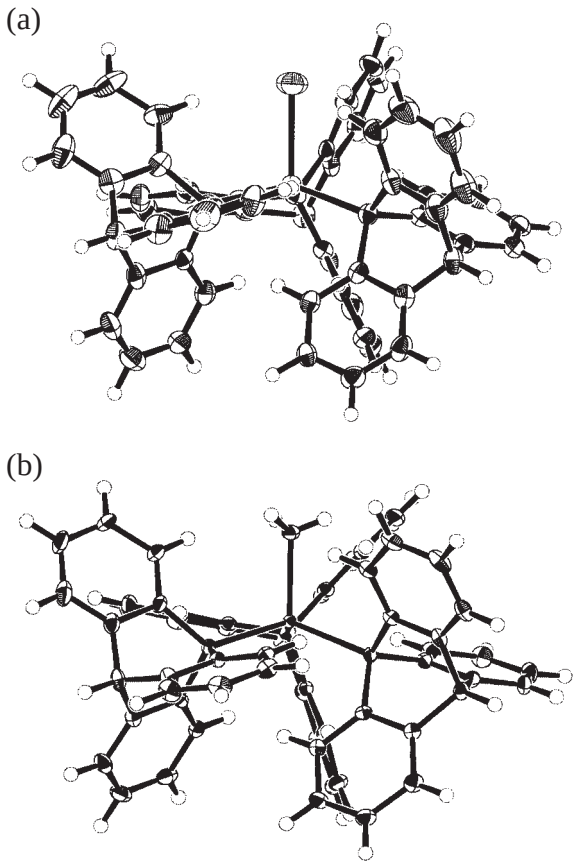

Fig. 1. The perspective drawings of X-ray molecular structures of (a) compound **2** and (b) compound **5**, each in the *P* conformation.

Table 1. Representative Bond Lengths (Å), Bond Angles (°), and Dihedral Angles (°) Obtained by X-ray Crystallography and MM2 Calculations[a)]

Compd	X	Sn–x	C–Sn–C		b)	Sn–C	x–Sn–C	x–Sn–C–C′		
			b)					**A**	**B**	**C**
2	Br	2.528(1)	12	114.6(3)	1	2.318(9)	107.5(2)	30.7	−90.7	152.0
			13	115.0(3)	2	2.289(9)	98.1(2)	38.9	−80.0	161.0
			23	116.4(3)	3	2.328(9)	102.3(3)	24.8	−95.0	146.9
			average	115.3		2.312	102.6	31.5	−88.6	153.3
		2.528		*115.0*		*2.223*	*103.0*	*31.7*	*−89.4*	*152.0*
5	CH_3	2.173(5)	12	113.7(2)	1	2.318(5)	108.0(2)	30.7	−88.8	150.3
			13	112.6(2)	2	2.291(5)	101.2(2)	38.9	−79.0	159.7
			23	116.0(2)	3	2.329(5)	103.6(2)	28.6	−91.7	148.7
			average	114.1		2.313	104.3	32.7	−86.5	152.9
		2.161		*112.0*		*2.241*	*104.8*	*29.7*	*−89.5*	*150.5*
7	H	*1.688*		*114.9*		*2.184*	*102.3*	*27.8*	*−89.7*	*148.5*

a) x denotes the central atom in group X. C denotes the bridgehead carbon C^9 in a 9-triptycyl group, and C′ the carbon bonded to C^9. See text for **A**, **B**, and **C**. Values in italics are obtained by MM2 calculations. b) 1, 2, or 3 denotes an arbitrary numbering of the three Tp groups.

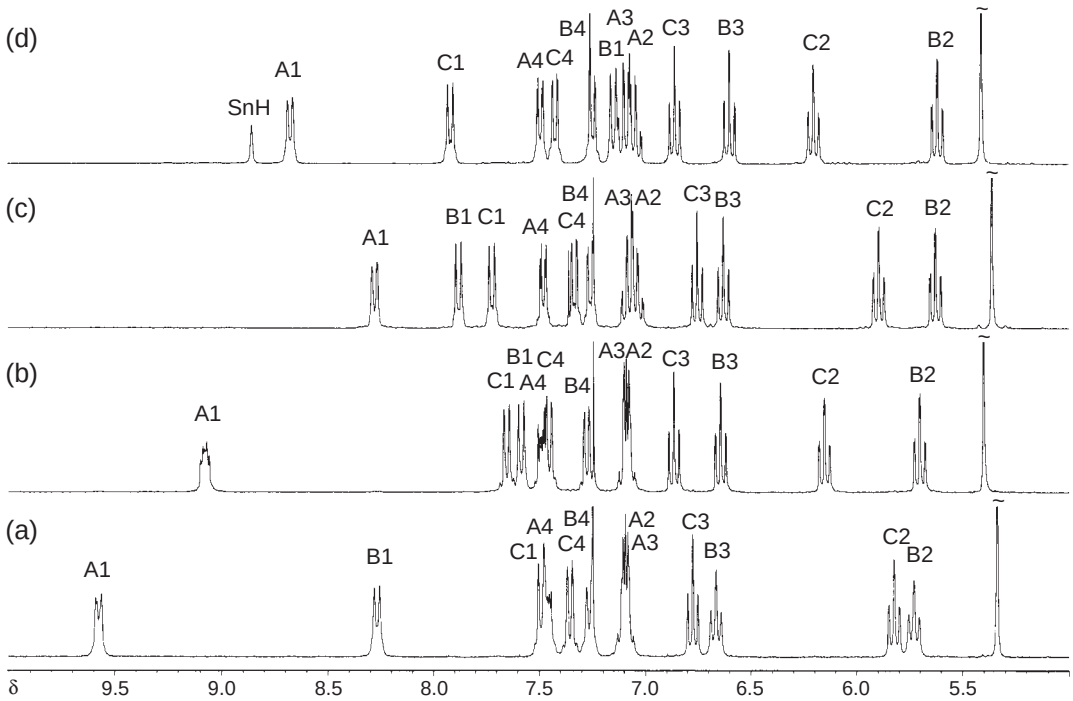

Fig. 2. The aromatic proton spectra of (a) compound **2**, (b) compound **4**, (c) compound **5**, and (d) compound **7**, in $CDCl_3$ at 22 °C with the signal assignments. Singlets at δ 5.3–5.4 are due to 10-H, and additional peaks at δ ca. 7.25 are due to $CHCl_3$.

er): the sites of these rings are hereafter referred to as **A**, **B**, and **C**, respectively (Table 1).

Molecular Mechanics Studies. Molecular mechanics calculations were performed using the MM2 program.[6] A set of parameters for tetrahedral tin by Horner and Newcomb[7] were incorporated and some still lacking parameters were added. Representative lengths and angles obtained by the calculations for compounds **2**, **5**, and **7** are included in Table 1.

The optimized structures for these compounds were of C_3 symmetry and similar to those obtained by X-ray crystallography mentioned above. Although the calculated bond lengths are significantly deviated from the observed ones probably due to the still poor Sn parameters, the bond angles and especially the dihedral angles around the Tp–Sn bonds are excellently reproduced. These results, together with the fact that these dihedral angles are almost independent of the substituent X, will indicate that the molecular structures and conformations are mainly governed by non-bonded interactions among the Tp groups.

NMR Analysis. At 22 °C, all the compounds examined except for the benzyl derivative **6** show twelve sharp signals for the Tp aromatic protons in the ^{1}H NMR spectra and 18 sharp signals for the Tp aromatic carbons in the ^{13}C NMR spectra, indicating that the three Tp groups are equivalent, while the three benzene rings in a Tp group are mutually nonequivalent. The ^{1}H NMR spectra in the aromatic region of several of the compounds are shown in Fig. 2 together with the signal assignments mentioned below. Compound **6** gives a broadened spectrum at 22 °C, but shows the same spectral features as mentioned above at low temperatures. These features indicate that the molecule in any compound adopts a conformation with C_3 symmetry and the conformational change is frozen on the NMR timescale.

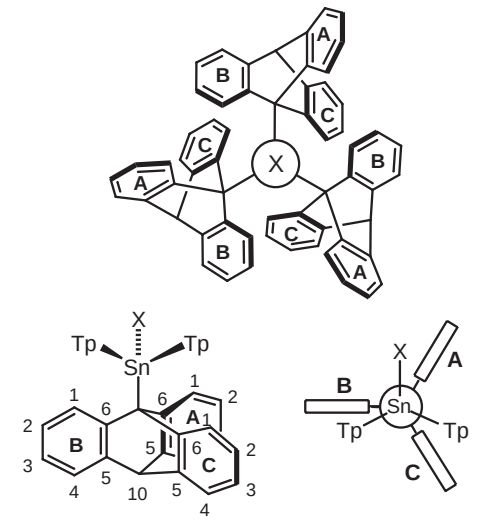

Scheme 1.

By assuming that the molecules in solution adopt a C_3 conformation similar to those found in the crystalline state or calculated by MM2, namely that three benzene rings of a Tp group, **A**, **B**, and **C**, have dihedral angles of ca. ±30, ∓90, and ±150°, respectively, with respect to the Sn–X bond (See Scheme 1 for the *P* conformer), twelve aromatic proton signals of the Tp moiety were unambiguously assigned on the basis of NOE and decoupling experiments (Table 2). The procedure will be described below for the methyl derivative **5** as a typical example.

Irradiation of the 10-H signal of **5** at δ 5.36 in $CDCl_3$ enhanced the intensity of three aromatic signals at δ 7.25, 7.33, and 7.47, which would naturally be assigned to either of A4,

Table 2. ^{1}H NMR Chemical Shifts in δ[a)]

Compd	**2**	**3**	**4**	**5**	**6**[b)]	**7**
X	Br	Cl	F	CH_3	CH_2Ph	H
A1	9.577	9.414	9.076[c)]	8.276	8.211	8.670
A2	7.102	7.100	7.079	7.035	6.698	7.025
A3	7.088	7.088	7.094	7.073	7.010	7.086
A4	7.451	7.465	7.487	7.471	7.470	7.484
B1	8.268	8.151	7.582	7.878	7.938	7.146
B2	5.729	5.718	5.700	5.622	5.702	5.612
B3	6.663	6.659	6.640	6.618	6.687	6.591
B4	7.260	7.268	7.274	7.249	7.312	7.241
C1	7.490	7.524	7.650	7.719	7.760	7.914
C2	5.822	5.888	6.152	5.890	5.890	6.197
C3	6.774	6.796	6.863	6.740	6.777	6.851
C4	7.355	7.380	7.451	7.325	7.364	7.415
10	5.338	5.352	5.400	5.356	5.422	5.405
X				2.177	4.322, 4.553[d)]	8.857
				(43.3)	(49.6)	(1614)

a) Obtained at 22 °C unless otherwise stated. Interproton coupling constants are not shown. Values in parentheses are ^{119}Sn–H coupling constants in Hz. b) Obtained at −29 °C. $^{2}J_{H-H}$ for the methylene protons is 15.6 Hz. c) $J_{H-F} = 3.6$ Hz. d) Methylene protons.

B4, or C4. Decoupling experiments easily revealed three sets of the four adjacent protons. Irradiation of the methyl signal at δ 2.18 enhanced the aromatic signal at δ 8.28, and this signal was assigned to A1 because this was the only hydrogen close to the methyl group (the distance between A1 and the methyl carbon is 2.405, 2.466, or 2.500 Å by X-ray crystallography and 2.431 Å by MM2). Irradiation of A1 enhanced the methyl signal and the signal at δ 7.88, so this aromatic signal was assigned to B1, because the B1 hydrogen on a flanking Tp group is located close to A1 (the distance between A1 and B1 is 2.339 Å by MM2). In this way, the twelve aromatic signals of **5** were completely assigned with no contradiction as given in Table 2.

Similarly, for compounds **6** and **7**, irradiation of the proton(s) in the X group (CH_2 in **6** or Sn–H in **7**) afforded the NOE enhancement of the signal at the lowest field in the aromatic region, which was assigned to A1 for each compound. For the fluoro compound **4**, the lowest field signal at δ 9.08 showed an additional splitting ($J = 3.6$ Hz) assignable to a through-space coupling with the ^{19}F nucleus,[8,9] indicating the proximity of this proton and the fluorine, and therefore this signal was assigned to A1. For compounds **2** and **3**, the lowest-field signal was reasonably assigned to A1, although no experimental confirmation was available. The assigned chemical shifts are compiled in Table 2.

In the ^{13}C NMR spectra, all the 18 aromatic carbons of the Tp moieties were separately observed and could mostly be assigned (Table 3). The assignments were made as follows. The CH-COSY experiments easily enabled the assignments of the tertiary carbon signals. For the quaternary carbons, those showing large C–Sn couplings ($J = 34$–53 Hz) were assigned to those at position 5 (A5, B5, or C5) and those with smaller couplings ($J < 14$ Hz) to those at position 6 (A6, B6, or C6), on the basis of the report that, while coupling constants between Sn and aromatic carbons in benzylstannanes are highly dependent on the stereochemical relationship between the relevant nuclei, $^{3}J_{C-Sn}$ is larger than $^{2}J_{C-Sn}$ in 9-trimethylstannyl-9,10-dihydro-9,10-ethanoanthracene (34.1 and 5.9 Hz, respectively).[10] The assignments to A, B, or C were made on the basis of the signal broadening: carbons (as well as hydrogens) on ring B gave the broadest signal and those on ring C gave the sharpest one at an appropriate temperature range, as discussed later in detail. The assignments from the signal broadening did not contradict with those from the CH-COSY studies for the tertiary carbons.

In the fluorine compound **4**, many carbons showed detectable couplings with ^{19}F: the bridgehead carbons (9-C), C5 and C6 carbons, and the ring-A carbons except for A4 (Table 3). Most of them will be ascribed mainly to a through-bond mechanism, but the large coupling of the A1 carbon ($J = 21.0$ Hz) will be due mainly to a through-space mechanism. As for the $^{3}J_{C-F}$ couplings with the A6, B6, and C6 carbons, a Karplus-type stereochemical relationship seems to hold (J of 2.7, ~0, and 1.7 Hz for the dihedral angles of 30, 90, and 150°, respectively).

It has been documented that tetra-coordinate halostannanes adopt a penta-coordinate trigonal-bipyramidal geometry in basic solvents such as pyridine, dimethyl sulfoxide (DMSO), and hexamethylphosphoric triamide (HMPA) by coordination of a solvent molecule to the tin atom.[11,12] The coordination is exemplified by a high-field shift of the ^{119}Sn signal, a low-field shift of the carbon signal directly bound to Sn, and the increase in the $^{1}J_{Sn-C}$ value upon changing the solvent from $CDCl_3$ to a basic solvent. For example, bromotriphenylstannane showed δ_{Sn}, δ_C, and $^{1}J_{Sn-C}$ (Hz) of −59.8, 136.9, and 595.0, respectively, in $CDCl_3$, and −228.4, 143.84, and 793.0, respectively, in DMSO-d_6.[11] In order to study whether such an effect operates in the Tp_3SnX compounds, NMR spectra were measured in DMSO-d_6, but no significant solvent effects were observed. For example, in the bromo compound **2**, δ_{Sn} were −43.6 and

Table 3. ^{13}C Chemical Shifts (δ) and C–Sn/C–F Coupling Constants (Hz) for Compounds **2**–**7**[a)]

Carbon	**2** (X = Br)		**3** (X = Cl)		**4** (X = F)		**5** (X = CH_3)		**6** (X = CH_2Ph)[b)]		**7** (X = H)	
	δ	J	δ	J	δ	J	δ	J	δ	J	δ	J
A1	129.06	26	128.94	25	128.82	—, *21.0*	128.32	24	129.05		128.62	51
A2	123.99	—	124.27	—	125.14	—, *1.7*	123.88	—	c)		124.68	—
A3	125.25	—	125.33	—	125.63	—, *1.0*	125.18	—	124.99		125.60	—
A4	123.70	9	123.69	10	123.55	9	123.91	8	c)		123.83	8
A5	147.69	44, 41	147.59	41	147.10	45, *0.5*	148.55	38	147.76[d)]		147.53	35, 34
A6	147.81	14	147.70	14	147.36	13, *2.7*	148.66	—	147.20[d)]		145.31	3
B1	128.89	37	128.94	33	128.91	29	129.56	29	129.61		129.18	25
B2	123.06	—	123.05	—	123.00	—	122.67	—	c)		122.76	—
B3	125.34	—	125.28	—	124.99	—	124.88	—	124.85		124.61	—
B4	122.92	9	122.94	9	123.02	9	122.74	7	c)		122.76	8
B5	146.55	47, 44	146.70	46	147.01	46	147.24	37	146.85[d)]		147.35	39, 38
B6	144.68	7	144.55	7	144.49	7	145.64	4	145.52[d)]		145.68	7
C1	129.82	45	129.52	47	128.54	48	131.24	27	131.06		130.27	30
C2	122.98	—	123.08	—	123.66	—	123.08	—	c)		123.83	—
C3	125.89	—	125.94	—	126.05	—	125.38	—	125.19		125.72	—
C4	123.27	13	123.39	13	123.85	13	122.90	7	c)		123.37	9
C5	146.39	53, 50	146.55	53, 51	146.83	51, *0.7*	146.40	37	146.04[d)]		146.40	41, 40
C6	143.87	10	143.95	11	144.36	11, *1.7*	145.41	4	145.45[d)]		148.24	8
9	79.86	403, 385	80.25	416, 398	76.92	437, 418, *8.1*	73.54	389, 372	75.65	356, 341	68.52	429, 410
10	55.12	7	55.18	8	55.27	6	55.51	5	54.91	—	55.37	4
α							12.04	226	35.28	234, 223		
i									139.23	31, 29		
o									132.01	40		
m									127.90	—		
p									125.31	6		

a) Measured at 22 °C unless otherwise stated. J_{C-Sn} values are given in plain type and J_{C-F} values in italic type. Where two J_{C-Sn} values are cited, the former is for ^{119}Sn and the latter is for ^{117}Sn. Where one J_{C-Sn} value is cited, the difference due to the isotopes is not observed. "—" means that J_{C-Sn} is not detected. b) Chemical shifts were measured at −29 °C, while J values were measured at 22 °C where cited. J values for the Tp aromatic carbons were not obtained. c) Appeared at δ 122.4–123.6 and could not be assigned. d) Tentatively assigned.

−34.8 in $CDCl_3$ and DMSO-d_6, respectively, and δ_C for the bridgehead carbon (C^9) of the Tp moiety were 79.86 and 79.62, respectively. These data indicate that no significant coordination of the solvent molecule takes place in DMSO. Such absence of coordination will be ascribed to the steric hindrance of coordination by the three bulky Tp groups.

Dynamic NMR Studies. When the temperature was elevated, the aromatic signals of the Tp moiety showed broadening and coalescence in all compounds, although the fast-exchange-limit spectra were not obtained even at the highest temperature examined (ca. 140 °C). ^1H NMR spectra of the methyl compound **5** in 1,1,2,2-tetrachloroethane-d_2 (TCE) at several temperatures are shown in Fig. 3 as a typical example. These lineshape changes will reasonably be ascribed to the conversion of one C_3 conformer to its enantiomeric conformer by rotation of the Tp–Sn bonds, a process hereafter referred to as enantiomerization (Scheme 2).

Although lineshape analysis of the aromatic proton signals should afford the rate constants for the enantiomerization, it did not seem so straightforward because the lineshape changes are deeply affected by the mechanistic details of the site exchange. So the discussion will start with compound **6** that carries a benzyl group as the direct probe for the enantiomerization. The methylene protons of the benzyl group in **6** will be diastereotopic and thus anisochronous if the enantiomerization is frozen on the NMR timescale, affording an AB-quartet signal. As the enantiomerization becomes faster, the signal will broaden, coalesce, and finally afford a sharp single peak. This was actually observed in variable temperature NMR experiments. The temperature dependence of the methylene signals is shown in Fig. 4. The spectra are somewhat complicated by the presence of the Sn-coupled signals, but the lineshapes were excellently reproduced by simulations using the DNMR5 program.[13] The best-fit theoretical spectra are also shown in Fig. 4. The least-squares analysis of the Eyring plot gave the kinetic parameters shown in Table 4. It should be noticed that these data were obtained without a knowledge of the mechanistic details of the enantiomerization.

Now the discussion goes back to the lineshape analysis of the aromatic proton signals. When the enantiomerization is slow, the three benzene rings of the Tp moiety are nonequivalent, and they become indistinguishable as the enantiomerization becomes fast on the NMR timescale. The lineshape changes are described in terms of three-site exchange, e.g., among A1, B1, and C1, and thus three independent rate constants are fundamentally necessary: those for the A1 → B1, A1 → C1, and B1 → C1 processes. The reverse processes (e.g., B1 → A1) naturally have the same rate constants as

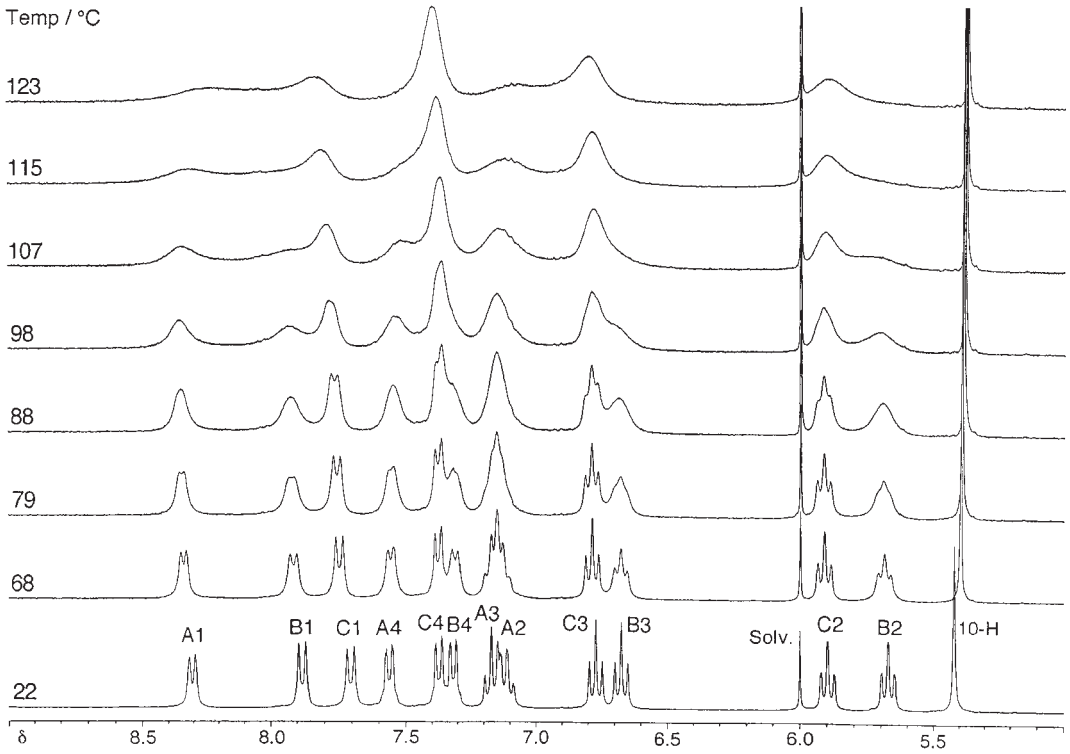

Fig. 3. The aromatic proton spectra of compound **5** in 1,1,2,2-tetrachloroethane-d_2 at various temperatures.

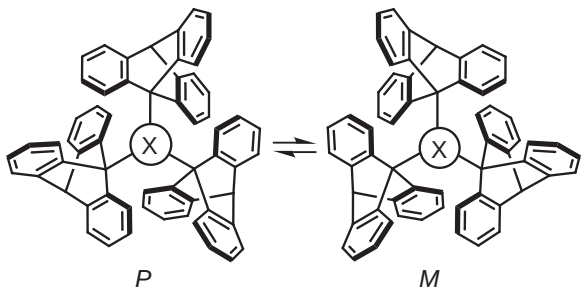

Scheme 2.

the respective forward processes because the three sites have the same populations. As explained in the next paragraph, a simple relationship holds among these three rate constants.

For simplicity, the molecules are assumed to exist in conformations with the dihedral angles of ± 30, ∓ 90, and $\pm 150^\circ$ between the Sn–X bond and the respective benzene ring plane as mentioned above. Small deviations of the dihedral angles from these values do not affect the discussion below. The enantiomerization then requires simultaneous rotation of the three Tp–Sn bonds by 60° in either direction. Two modes of rotation are possible for one Tp–Sn bond as shown in Scheme 3: The indicated Tp group of the left conformer (*P*) in Scheme 3 rotates either clockwise (*mode i*) or anticlockwise (*mode ii*). In *mode i*, the gray benzene ring originally at site **A** moves to site **B** by 60° rotation, the blank one at site **B** moves to site **A**, while the dark one at site **C** does not change its site. In this mode, any benzene ring does not eclipse the Sn–X or Sn–Tp bond during the rotation. In *mode ii*, the blank benzene ring at site **B** moves to site **C**, the dark one at site **C** moves to site **B**, but the gray one at site **A** does not change its site. In this mode all the benzene rings eclipse the Sn–X or Sn–Tp bond during the rotation. Therefore, sites **A** and **B** exchange by *mode i*, sites **B** and **C** exchange by *mode ii*, but direct exchange between **A** and **C** never occurs by either mode.

In the enantiomerization of a molecule of the present compounds, each of the three Tp–Sn bonds rotates either by *mode i* or *mode ii*, and therefore there are four possible combinations of modes: (a) *i*, *i*, *ii*; (b) *i*, *ii*, *ii*; (c) *i*, *i*, *i*; and (d) *ii*, *ii*, *ii*. In Mechanism (c), all Tp–Sn bonds rotate by *mode i*, and thus site **C** should never move to the other sites. This means that the signals of the protons at this site should remain sharp irrespective of the temperature, which contradicts the observed NMR lineshapes. Therefore, Mechanism (c) is rejected. Similarly Mechanism (d) is also rejected, because site **A** should never move to the other sites in this mechanism.

In Mechanism (a), the exchange between site **A** and site **B** (*mode i*) takes place twice as often as the exchange between site **B** and site **C** (*mode ii*), and the direct exchange between site **A** and site **C** never occurs. The enantiomerization rate is determined by the lifetime of the most frequently exchanging site, i.e., site **B** in this case, and the rate constant for the enantiomerization, k_e, is given by the sum of the rate constants $k(\mathbf{B} \rightarrow \mathbf{A})$ and $k(\mathbf{B} \rightarrow \mathbf{C})$, where $k(\mathbf{B} \rightarrow \mathbf{A}) = 2k(\mathbf{B} \rightarrow \mathbf{C})$ as discussed above. Thus $k_e = 3k(\mathbf{B} \rightarrow \mathbf{C}) = 3k(\mathbf{B} \rightarrow \mathbf{A})/2$. Therefore, a simple relationship holds among the rate constants for the site exchange in terms of the rate constant for the enantiomerization, k_e, as given in Scheme 4(a). If Mechanism (b) operates, the rate constants for the site exchange will be as shown in Scheme 4(b).

Qualitatively, Mechanism (a) predicts that a signal due to a proton on the ring **B** (Signal B) will be the broadest, Signal C the sharpest, and Signal A intermediate among a set of three

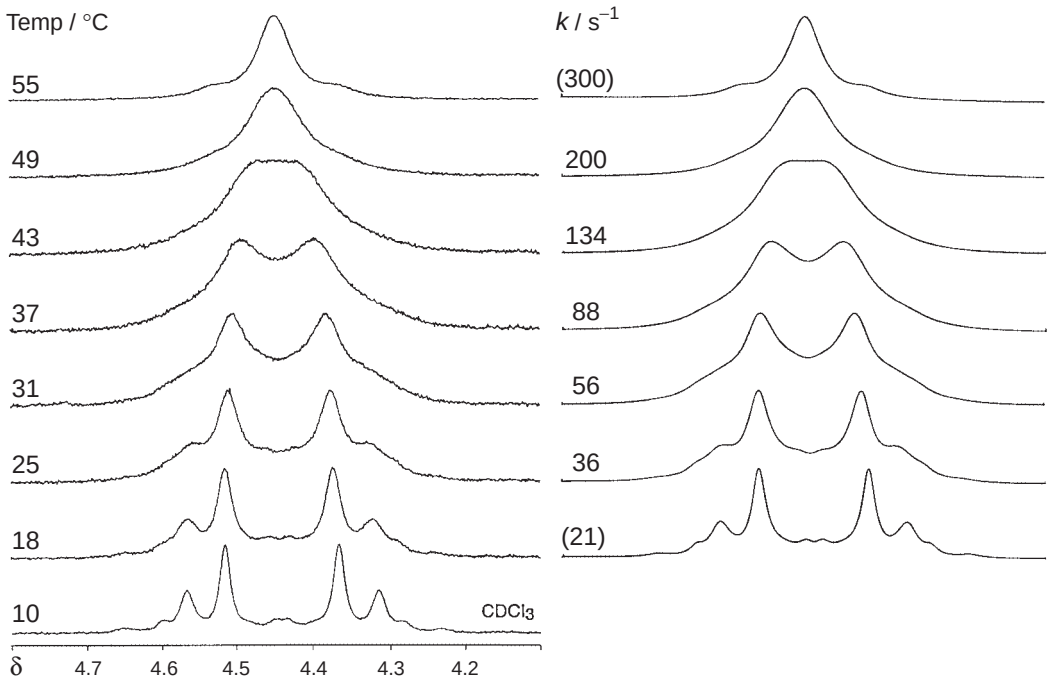

Fig. 4. The observed methylene proton signals of compound **6** in $CDCl_3$ at various temperatures (left), and the calculated spectra with best-fit rate constants (right). Rate constants in parentheses mean that the spectra were calculated based on the data given in Table 6.

Table 4. Free Energies of Activation and Rate Constants for the Enantiomerization at 350 K in TCE and DMSO

Compd	X	TCE		DMSO	
		$\Delta G^{\ddagger}$ (350 K) / kJ mol^{-1}	k (350 K) / s^{-1}	$\Delta G^{\ddagger}$ (350 K) / kJ mol^{-1}	k (350 K) / s^{-1}
2	Br	70.5	220	67.9	550
3	Cl	71.3	170	69.2	340
4	F	76.8	25	78.1	16
5	CH_3	77.2	22	75.4	41
6	CH_2Ph	65.9[a)]	1.1×10^3[a)]		
		64.3[a,b)]	40[a,b)]		
7	H	81.6	4.9		
1	Cl	84.1	2.1		

a) Solvent: $CDCl_3$. b) At 300 K.

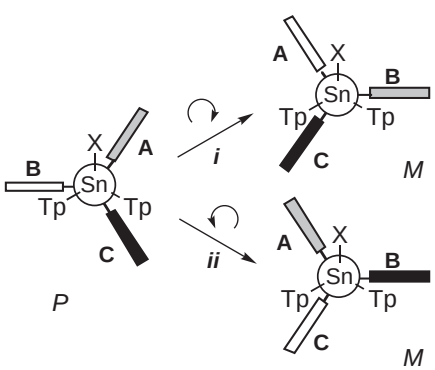

Scheme 3.

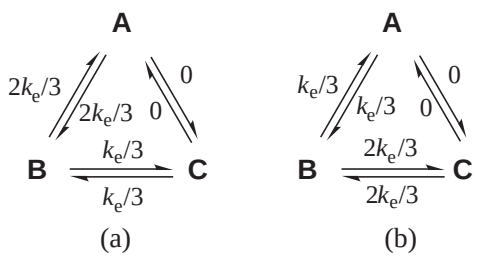

Scheme 4.

signals when the enantiomerization takes place at a moderate rate on the NMR timescale, while Signal A will be the sharpest when Mechanism (b) operates. The spectra in Fig. 3, for exam-

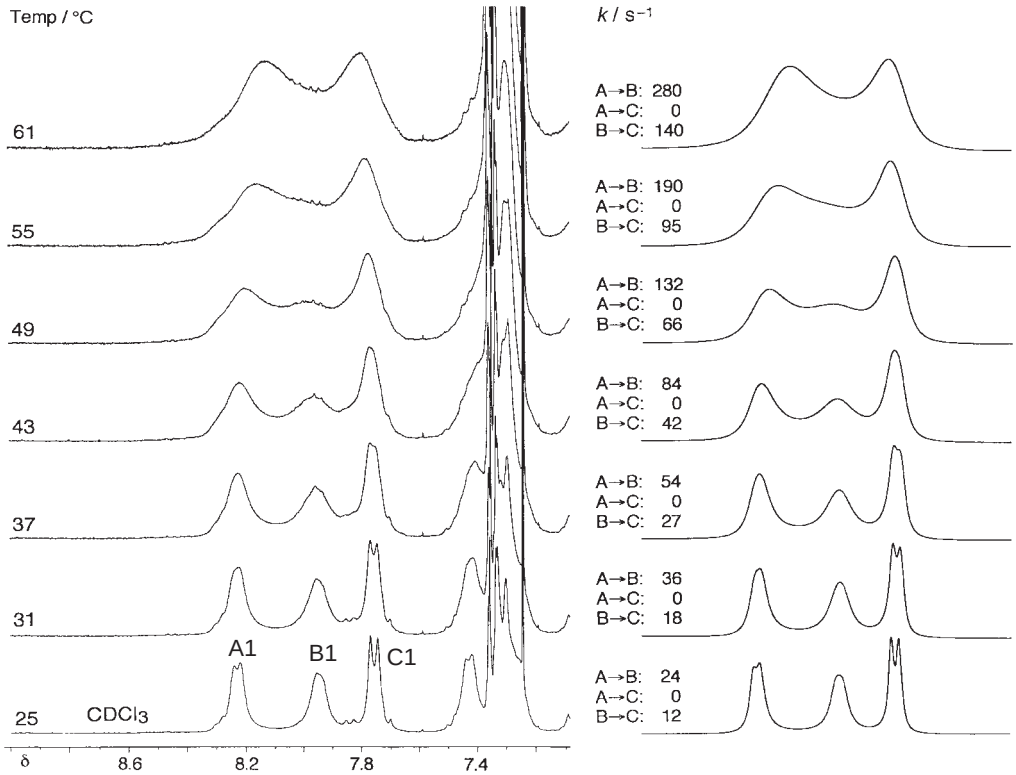

Fig. 5. The observed peri-proton signals of compound **6** in $CDCl_3$ at various temperatures (left), and the calculated spectra with best-fit rate constants (right).

ple, seem to agree better with Mechanism (a).

On the basis of the discussion above, the temperature-dependent lineshapes of the aromatic proton signals of compound **6** were analyzed using the DNMR3 program.[14] Calculations assuming Mechanism (a) excellently reproduced the experimental spectra. The observed and calculated spectra of the peri protons (A1, B1, and C1) are shown in Fig. 5. The kinetic parameters obtained are given in Table 3; these values are in excellent agreements with those obtained from the analysis of the methylene proton signals. This shows that the relationship in Scheme 4(a) and thus the enantiomerization mechanism mentioned above are valid. Although the possibility of small contamination of Mechanism (b) can not be ruled out, it can be safely said that the extent of contamination is too small to affect the lineshape.

Preference for Mechanism (a) will be understood as follows. Two of the three Tp–Sn bonds would disrotate in a bevel gear fashion, and thus one bond rotates in *mode i* and the other in *mode ii*. *Mode i* would have a lower energy barrier than *mode ii*, because the former mode does not require the eclipsing of the benzene rings with the Sn–X or Sn–Tp bonds during the rotation. Therefore, the third Tp–Sn bond would prefer *mode i*.

Qualitatively, the signal due to a nucleus (^1H or ^{13}C) in site C is the sharpest, that in site B is the broadest, and that in site A is intermediate, as typically shown in spectra at 68–88 °C in Fig. 3 and those at 25–37 °C in Fig. 5. This feature enabled the assignments of the quaternary carbons as mentioned before (Table 3).

Since the methodology for determining the enantiomerization rate constants from the lineshape analysis of the aromatic signals was established, this was applied to the compounds lacking the potential diastereotopic groups in the X moiety of Tp_3SnX, namely, **2**, **3**, **4**, **5**, and **7**, as well as to the germane reported by Mislow and co-workers,[2] Tp_3GeCl (**1**). Temperature dependent ^1H NMR spectra were obtained for these compounds in TCE, except for compound **6** where chloroform-*d* was used, and also in DMSO-d_6. The lineshapes of the aromatic signals were analyzed as mentioned above, and the Eyring plots of the obtained rate constants afforded the activation parameters. The data are shown in Table 6 in the Experimental Section, where the temperature ranges and the signals used for the analysis are also included. The $\Delta G^{\ddagger}$ and k values at 350 K calculated from the parameters given in Table 6 are compiled in Table 4.

Table 4 reveals several aspects worth consideration. For one thing, the energy barrier to enantiomerization decreases on going from **7** to **5** to **6** in the order of increasing steric demand of the group X. This indicates that the transition state for enantiomerization is destabilized to a lesser extent than the ground state upon replacing X by a bulkier group. A similar tendency was also observed in the halogen compounds **2**, **3**, and **4**: the bulkier the halogen, the lower the barrier. However, **5** has a significantly higher barrier than **3** and **4**, though the effective van der Waals radius of CH_3 (1.80 Å[15]) is similar to those of Cl and Br (1.73 and 1.86 Å, respectively[15]). This may be understood by taking into account the ease of the Sn–halogen bond elongation. A C–X bond (X = Cl or Br) has a smaller stretching force constant than a C–C bond as shown by the MM2 parameters, and so it will be reasonable to assume that a Sn–X bond (X = Cl or Br) has a smaller stretching force constant than a Sn–C bond. When the Sn–X bond is elongated at the transition state for enantiomerization, the Tp–Sn–Tp an-

gles can more easily open up, and thus the destabilization of the transition state will be smaller than in the cases where the bond elongation is not easily expected, resulting in the lowering of the barrier.

Extrapolation of the kinetic data for **1** in Table 6 gives $k = 1.7 \times 10^{-5}$ s^{-1} at -29 °C for the enantiomerization. This value is compared with $k = 2.67 \times 10^{-5}$ s^{-1} calculated from the racemization rate in methanol reported by Mislow and coworkers. If the difference in the solvent used and in the temperature range of the measurements is allowed for, these values are considered to agree very well. This agreement also will support the validity of finding the racemization rate constants from the lineshape analysis of the aromatic proton signals.

Experimental

General. Melting points are not corrected. ^{1}H, ^{13}C, and ^{19}F NMR spectra were obtained on a Bruker ARX-300 spectrometer operating at 300.1 MHz for ^{1}H, 75.4 MHz for ^{13}C, and 282.4 MHz for ^{19}F, respectively. Chemical shifts are referenced with internal tetramethylsilane ($\delta_H = 0.00$), $CDCl_3$ ($\delta_C = 77.00$), and C_6F_6 ($\delta_F = -163.0$). The ^{13}C NMR spectral data are compiled in Table 3. In variable-temperature experiments, temperatures were calibrated using a methanol sample or an ethylene glycol sample and are reliable to ±1 °C. ^{119}Sn NMR spectra were obtained on a JEOL JNM-EX270 at 100.50 MHz or on a JEOL JNM-EX400 at 148.95 MHz, and chemical shifts are referenced with external Me_4Sn ($\delta = 0.00$). Preparative gel permeation chromatography (GPC) was performed on an LC-908 Liquid Chromatograph (Japan Analytical Industry Co., Ltd.) using a series of JAIGEL 1H and 2H columns and chloroform as the eluent.

Bromotris(9-triptycyl)stannane (2). To a suspension of 3.33 g (10.0 mmol) of 9-bromotriptycene in 60 mL of diethyl ether was added 6.7 mL (10.0 mmol) of butyllithium in hexane (1.58 mol L^{-1}), and the mixture was stirred at room temperature for 4 h. The supernatant solvent was decanted off, and the residue was washed several times with diethyl ether, and then was suspended in 120 mL of diethyl ether. To the stirred suspension was added 0.33 mL (2.5 mmol) of $SnBr_4$ and the mixture was stirred for 32 h at room temperature. After quenching with water, the solids were collected by filtration to give 1.85 g (1.93 mmol, 77%) of **2**, mp 370 °C (dec). Found: C, 75.35; H, 3.89%. Calcd for $C_{60}H_{39}BrSn$: C, 75.18; H, 4.10%. ^{1}H NMR ($CDCl_3$) δ 5.338 (3H, s, 10-H), 5.729 (3H, t, $J = 7.3$ Hz, B2), 5.822 (3H, td, $J = 7.6$, 1.1 Hz, C2), 6.663 (3H, t, $J = 7.3$ Hz, B3), 6.774 (3H, t, $J = 7.3$ Hz, C3), 7.088 (3H, m, A3), 7.102 (3H, m, A2), 7.260 (3H, d, $J = 7.0$ Hz, B4), 7.355 (3H, d, $J = 7.1$ Hz, C4), 7.451 (3H, m, A4), 7.490 (3H, d, $J = 7.6$ Hz, C1), 8.268 (3H, d, $J = 7.6$ Hz, B1), 9.577 (3H, m, A1). ^{119}Sn NMR ($CDCl_3$) δ −43.6.

Chlorotris(9-triptycyl)stannane (3). To a stirred solution of 200 mg (0.208 mmol) of **2** and 1.1 mL (6.3 mmol) of hexamethylphosphoric triamide in 20 mL of dry tetrahydrofuran at −78 °C under Ar was added 0.45 mL (0.63 mmol) of *t*-butyllithium in pentane (1.40 mol L^{-1}), and the mixture was stirred at this temperature for 2 h. To this solution was added 0.10 mL (1.46 mmol) of sulfuryl chloride, and the solution was left to warm up to room temperature. After addition of 10 mL of water, the mixture was extracted with diethyl ether. The extracts were dried over $MgSO_4$ and evaporated. The residue was recrystallized from $CHCl_3$ to give 153 mg (1.70 mmol, 80%) of **3**, mp 360–370 °C (dec). Found: C, 78.50; H, 4.33%. Calcd for $C_{60}H_{39}ClSn$: C, 78.84; H, 4.30%. ^{1}H NMR ($CDCl_3$) δ 5.352 (3H, s, 10-H), 5.718 (3H, td, $J = 7.6$, 0.9 Hz, B2), 5.888 (3H, td, $J = 7.6$, 1.1 Hz, C2), 6.659 (3H, t, $J = 7.3$ Hz, B3), 6.796 (3H, t, $J = 7.3$ Hz, C3), 7.088 (3H, m, A3), 7.100 (3H, m, A2), 7.268 (3H, d, $J = 7.4$ Hz, B4), 7.380 (3H, dd, $J = 7.2$, 0.9 Hz, C4), 7.465 (3H, m, A4), 7.524 (3H, d, $J = 7.6$ Hz, C1), 8.151 (3H, d, $J = 7.6$ Hz, B1), 9.412 (3H, m, A1). ^{119}Sn NMR ($CDCl_3$) δ −1.2.

Fluorotris(9-triptycyl)stannane (4). To a solution of 200 mg (0.208 mmol) of **2** in 20 mL of benzene was added 24 mg (0.416 mmol) of KF and 11 mg (0.042 mmol) of 18-crown-6, and the mixture was heated under reflux for 24 h. GPC of the residual mass followed by recrystallization from chloroform–hexane afforded 156 mg (0.174 mmol, 84%) of **4**, mp 407–409 °C (dec). Found: C, 80.41; H, 4.40%. Calcd for $C_{60}H_{39}FSn$: C, 80.28; H, 4.38%. ^{1}H NMR ($CDCl_3$) δ 5.400 (3H, s, 10-H), 5.700 (3H, td, $J = 7.6$, 1.3 Hz, B2), 6.152 (3H, td, $J = 7.6$, 1.2 Hz, C2), 6.640 (3H, td, $J = 7.5$, 0.8 Hz, B3), 6.863 (3H, t, $J = 7.3$ Hz, C3), 7.03–7.13 (6H, m, A2 and A3), 7.274 (3H, dd, $J = 7.2$, 1.1 Hz, B4), 7.451 (3H, dd, $J = 7.3$, 1.1 Hz, C4), 7.487 (3H, m, A4), 7.582 (3H, d, $J = 7.6$ Hz, B1), 7.650 (3H, d, $J = 7.4$ Hz, C1), 9.076 (3H, m, A1). The A1 signal appeared as a doublet ($J = 3.6$ Hz) upon irradiation of the A2/A3 signal at δ 7.08. ^{119}Sn NMR ($CDCl_3$) δ 30.4 ($^1J_{Sn-F} = 2564$ Hz). ^{19}F NMR ($CDCl_3$) δ −172.5 ($^1J_{^{119}Sn-F} = 2565$ Hz, $^1J_{^{117}Sn-F} = 2451$ Hz).

Methyltris(9-triptycyl)stannane (5). To a stirred solution of 200 mg (0.209 mmol) of bromotris(9-triptycyl)stannane (**2**) and 0.15 mL (0.84 mmol) of hexamethylphosphoric triamide (HMPA) in 30 mL of THF at −78 °C was added 0.52 mL (0.84 mmol) of *t*-butyllithium in pentane (1.60 mol L^{-1}) and the mixture was stirred for 2 h at this temperature. To the solution was added 0.91 mL (14.6 mmol) of methyl iodide and the mixture was allowed to warm up to room temperature. After quenching with water, the solvent was removed by evaporation at reduced pressure. Column chromatography on silica gel with dichloromethane as the eluent followed by GPC gave 120 mg (0.134 mmol, 64%) of **5**, mp 386 °C (dec). Found: C, 81.93; H, 4.97%. Calcd for $C_{61}H_{42}Sn$: C, 81.98; H, 4.74%. ^{1}H NMR ($CDCl_3$) δ 2.177 (3H, s, $^2J_{Sn-H} = 43.3$ Hz, CH_3), 5.356 (3H, s, 10-H), 5.622 (3H, td, $J = 7.6$, 1.2 Hz, B2), 5.890 (3H, td, $J = 7.6$, 1.1 Hz, C2), 6.618 (3H, t, $J = 7.1$ Hz, B3), 6.740 (3H, t, $J = 7.0$ Hz, C3), 7.073 (3H, m, A3), 7.035 (3H, m, A2), 7.249 (3H, td, $J = 7.1$, 1.0 Hz, B4), 7.325 (3H, td, $J = 7.2$, 1.0 Hz), 7.471 (3H, dd, $J = 6.8$, 1.8 Hz, A4), 7.719 (3H, d, $J = 7.6$ Hz, C1), 7.878 (3H, d, $J = 7.6$ Hz, B1), 8.276 (3H, d, $J = 7.0$ Hz, A1). ^{119}Sn NMR ($CDCl_3$) δ −59.4.

Benzyltris(9-triptycyl)stannane (6). To a stirred solution of 1.00 g (1.04 mmol) of bromotris(9-triptycyl)stannane (**2**) and 0.55 mL (3.13 mmol) of HMPA in 150 mL of THF at −78 °C was added 2.11 mL (3.13 mmol) of *t*-butyllithium in pentane (1.48 mol L^{-1}) and the mixture was stirred for 2 h at this temperature. To the solution was added 0.62 mL (5.12 mmol) of benzyl bromide and the mixture was allowed to slowly warm up to room temperature. After quenching with water, the solvent was removed by evaporation at reduced pressure. Column chromatography on silica gel with dichloromethane as the eluent followed by GPC gave 296 mg (0.305 mmol, 29%) of **6**, mp 295 °C (dec). Found: C, 83.30; H, 4.88%. Calcd for $C_{67}H_{46}Sn$: C, 82.98; H, 4.78%. ^{1}H NMR ($CDCl_3$, −29 °C) δ 4.322 (1H, d, $J = 15.6$ Hz, $^2J_{Sn-H} = 49.6$ Hz), 4.553 (1H, d, $J = 15.6$ Hz, $^2J_{Sn-H} = 49.6$ Hz), 5.422 (3H, s, 10-H), 5.702 (3H, td, $J = 7.6$, 1.2 Hz, B2), 5.890 (3H, td, $J = 7.6$, 1.2 Hz, C2), 6.687 (3H, t, $J = 7.0$ Hz, B3), 6.698 (3H, td, $J = 7.6$, 1.2 Hz, A2), 6.777 (3H, t, $J = 7.4$ Hz, C3), 6.87–6.97 (3H, m, *m*- and *p*-H), 7.010 (3H, t, $J = 7.4$ Hz, A3), 7.312 (3H, dd, $J = 7.2$, 1.1 Hz, B4), 7.36 (2H, m, *o*-H), 7.364

(3H, dd, $J = 7.3$, 1.2 Hz, C4), 7.470 (3H, dd, $J = 7.3$, 1.2 Hz, A4), 7.760 (3H, d, $J = 7.6$ Hz, C1), 7.938 (3H, d, $J = 7.6$ Hz, B1), 8.221 (3H, d, $J = 7.7$ Hz, A1). ^{119}Sn NMR ($CDCl_3$) δ −69.4.

Tris(9-triptycyl)stannane (7). To a stirred solution of 200 mg (0.208 mmol) of **2** in 20 mL of dry THF at 0 °C was added 85 mg (0.63 mg) of $AlCl_3$ and then 10 mg (0.26 mmol) of $LiAlH_4$ and the mixture was stirred for 24 h at room temperature. The mixture was quenched with water and extracted with diethyl ether. The extracts were washed with water, dried over $MgSO_4$, and evaporated. Recrystallization of the residue from chloroform gave 115 mg (0.131 mmol, 63%) of **7**, mp 300–320 °C (dec). Found: C, 81.96; H, 4.83%. Calcd for $C_{60}H_{40}Sn$: C, 81.92; H, 4.58%. ^{1}H NMR ($CDCl_3$) δ 5.405 (3H, s, 10-H), 5.612 (3H, td, $J = 7.6$, 1.3 Hz, B2), 6.197 (3H, td, $J = 7.6$, 1.3 Hz, C2), 6.591 (3H, td, $J = 7.5$, 0.9 Hz, B3), 6.851 (3H, td, $J = 7.4$, 0.7 Hz, C3), 7.025 (3H, td, $J = 7.4$, 1.5 Hz, A2), 7.086 (3H, td, $J = 7.3$, 1.1 Hz, A3), 7.146 (3H, d, $J = 7.6$ Hz, B1), 7.241 (3H, dd, $J = 7.2$, 1.2 Hz, B4), 7.415 (3H, dd, $J = 7.3$, 1.2 Hz, C4), 7.484 (3H, dd, $J = 7.1$, 1.4 Hz, A4), 7.914 (3H, d, $J = 7.5$ Hz, C1), 8.670 (3H, d, $J = 7.3$ Hz, A1), 8.857 (1H, s, $^1J_{Sn-H} = 1614$, 1543 Hz, Sn–H). ^{119}Sn NMR ($CDCl_3$) δ −246.2.

Molecular Mechanics Studies. Molecular mechanics calculations were performed employing the MM2 program[6] on an NEC EWS-4800/360 workstation. A set of parameters involving tetrahedral tin were incorporated according to Horner and Newcomb.[7] In addition, following parameters were newly added: Sn–Br: $K_e = 2.0$ mdyn Å^{-1}, $l_o = 2.53$ Å; Br–Sn–C(sp^3): $K_b = 0.43$ mdyn rad^{-2}, $\theta_o = 98.0°$; Br–Sn–C(sp^3)–C(sp^2): $V_3 = 0.066$ kcal mol^{-1}. These values were tentatively assigned based on the existing parameters in the force field and those in Ref. 7.

X-ray Crystallography. Crystals of compounds **2** and **5** grown from dichloromethane–hexane were used. The crystal data and the parameters for data collection, structure determination, and refinement are summarized in Table 5. Diffraction data were collected on a Rigaku AFC7R or a Rigaku/MSC Mercury CCD diffractometer and calculations were performed using the SHELXL97 program.[16] The structures were solved by direct methods followed by full-matrix least-squares refinement with all non-hydrogen atoms anisotropic and all hydrogen atoms isotropic. Reflection data with $|I| > 2.0\sigma(I)$ were used. The function minimized was $\Sigma w(|F_o| - |F_c|)^2$ where $w = [\sigma^2(F_o)]^{-1}$.

Crystallographic data have been deposited with Cambridge Crystallographic Data Centre: Deposition number CCDC-258285 and 226291 for compounds **2** and **5**, respectively. Copies of the data can be obtained free of charge via http//www.ccdc.cam.ac.uk/conts/retrieving.html (or from the Cambridge Crystallographic Data Centre, 12, Union Road, Cambridge, CB2 1EZ, UK; Fax: +44 1223 336033; e-mail: ordeposit@ccdc.cam.ac.uk).

Lineshape Analysis. Total lineshape analysis was performed by visual matching of experimental spectra with theoretical spectra computed on an NEC PC9821Xs personal computer equipped with a Mutoh PP-210 plotter. For the analysis of aromatic proton signals, the DNMR3K program, a modified version of the DNMR3 program[14] converted for use on personal computers by Dr. Hiroshi Kihara, was used, while the DNMR5 program[13] was used for the simulation of the methylene proton signals of compound **4**. Temperature dependences of chemical shift differences and T_2 values were properly taken into account. The enthalpies and entropies of activation obtained by the least-squares analysis of the Eyring plots of the rate constants are compiled in Table 6.

Table 5. Crystal Data and Parameters for Data Collection, Structure Determination, and Refinement

Compound	**2**	**5**
Empirical formula	$C_{60}H_{39}BrSn$	$C_{61}H_{42}Sn \cdot 2CHCl_3$
Formula weight	958.59	1132.48
Crystal system	tetragonal	orthorhombic
Space group	$P4_2/n$	$Pbca$
a/Å	27.7835 (2)	20.0474 (1)
b/Å	27.7835 (2)	21.7181 (2)
c/Å	13.2767 (2)	23.1934 (2)
V/Å^3	10248.6 (2)	10098.2 (1)
Z	8	8
D_c/g cm^{-3}	1.268	1.490
μ(Mo Kα)/cm^{-1}	0.7107	0.7107
Temp/K	180.1	130.2
$2\varphi_{max}$/°	54.5	54.5
No. of reflections measured		
Total	11605	11278
Unique	5125	7954
No. of refinement variables	560	632
Final R; R_w	0.0582; 0.0801	0.0474; 0.0983
GOF	1.877	1.210

$R = \Sigma||F_o| - |F_c||/\Sigma|F_o|$, R_w on F^2.

Table 6. Activation Parameters for the Enantiomerization

Compd	X	Solvent[a)]	$\Delta H^\ddagger$	$\Delta S^\ddagger$	Temp range[b)]	Obsd signals
			kJ mol^{-1}	J mol^{-1} K^{-1}	°C	
2	Br	TCE	68.1 ± 2.4	−6.9 ± 7.1	48–87	A1, B1; B2, C2, B3, C3
		DMSO	62.0 ± 0.9	−16.8 ± 2.7	32–75	A1, B1; B3, C3
3	Cl	TCE	66.3 ± 1.5	−14.3 ± 4.3	47–90	A1, B1; B2, C2
		DMSO	67.7 ± 0.7	−4.5 ± 2.2	39–75	A1, B1; B3, C3
4	F	TCE	67.5 ± 1.3	−26.7 ± 3.5	88–123	A1, B1, C1; B2, C2: B3, C3
		DMSO	76.8 ± 0.8	−3.5 ± 2.1	93–123	B2, C2
5	CH_3	TCE	75.3 ± 0.9	−5.3 ± 2.3	88–123	A1, B1, C1
		DMSO	72.6 ± 0.8	−8.0 ± 2.2	71–104	A1, B1; B3, C3
6	CH_2Ph	$CDCl_3$	54.5 ± 1.9	−32.5 ± 6.1	25–61	A1, B1, C1
			54.7 ± 0.8	−31.7 ± 2.6	25–49	CH_2
7	H	TCE	82.4 ± 1.9	2.6 ± 4.7	97–138	A1, C1; B2, C2
1	Cl	TCE	76.3 ± 2.3	−22.3 ± 5.7	112–142	A1, B1, C1

a) TCE: $CDCl_2CDCl_2$; DMSO: $(CD_3)_2SO$. b) The temperature range where the lineshape was analyzed.

We thank Dr. Kei Goto and Mr. Norikiyo Nakagawa, the University of Tokyo, for obtaining the ^{119}Sn spectra. This work was partially supported by a Grant-in-Aid for Scientific Research (No. 16550043) from the Japan Society of the Promotion of Science. The support of the Kitasato University Research Grant for Young Researchers (to M. M.) is also acknowledged.

References

This paper is dedicated to Professor Michinori Ōki on the occasion of his 77th birthday.

1 a) H. Iwamura, *J. Mol. Struct.*, **126**, 401 (1985). b) H. Iwamura and K. Mislow, *Acc. Chem. Res.*, **21**, 175 (1988). c) K. Mislow, *Chemtracts: Org. Chem.*, **2**, 151 (1989).

2 a) J. M. Chance, J. H. Geiger, and K. Mislow, *J. Am. Chem. Soc.*, **111**, 2326 (1989). b) J. M. Chance, J. H. Geiger, Y. Okamoto, R. Aburatani, and K. Mislow, *J. Am. Chem. Soc.*, **112**, 3540 (1990).

3 R. J. Ranson and R. M. G. Roberts, *J. Organomet. Chem.*, **107**, 295 (1976).

4 G. Yamamoto, M. Kaneko, M. Ohkuma, and M. Minoura, *Chem. Lett.*, **32**, 964 (2003).

5 For the usage of the *M*/*P* descriptors, see: R. S. Cahn, C. Ingold, and V. Prelog, *Angew. Chem., Int. Ed. Engl.*, **5**, 385 (1966).

6 N. L. Allinger and H. L. Flanagan, *J. Comput. Chem.*, **4**, 399 (1983).

7 J. H. Horner and M. Newcomb, *Organometallics*, **10**, 1732 (1991).

8 For the through-space mechanism in spin–spin coupling, see: J. Hilton and L. H. Sutcliffe, *Prog. NMR Spectrosc.*, **10**, 27 (1975).

9 For through-space ^{1}H–^{19}F couplings in triptycene derivatives, see: G. Yamamoto and M. Ōki, *J. Org. Chem.*, **49**, 1913 (1984); G. Yamamoto and M. Ōki, *Tetrahedron Lett.*, **26**, 457 (1985).

10 W. Adcock, B. D. Gupta, W. Kitching, and D. Doddrell, *J. Organomet. Chem.*, **102**, 297 (1975).

11 J. Holeček, M. Nádvorník, K. Handlíř, and A. Lyčka, *J. Organomet. Chem.*, **241**, 177 (1983).

12 J. Holeček, A. Lyčka, K. Handlíř, and M. Nádvorník, *Collect. Czech. Chem. Commun.*, **53**, 571 (1988).

13 D. S. Stephenson and G. Binsch, QCPE Program No. 365; QCMP Program No. 059.

14 D. A. Kleier and G. Binsch, QCPE Program No. 165.

15 G. Bott, L. D. Field, and S. Sternhell, *J. Am. Chem. Soc.*, **102**, 5618 (1980).

16 G. M. Sheldrick, "Program for the Refinement of Crystal Structures," University of Göttingen, Germany (1997).